OES Faculty Publications   Ocean & Earth Sciences

Preferential Depletion of Zinc Within Costa Rica Upwelling Dome Creates Conditions for Zinc Co-Limitation of Primary Production

P. Dreux Chappell
Old Dominion University

Jagruti Vedmati

Karen E. Selph

Heather A. Cyr

Bethany D. Jenkins

See next page for additional authors

Follow this and additional works at: https://digitalcommons.odu.edu/oeas_fac_pubs

Part of the Marine Biology Commons, and the Oceanography Commons

Authors

P. Dreux Chappell, Jagruti Vedmati, Karen E. Selph, Heather A. Cyr, Bethany D. Jenkins, Michael R. Landry, and James W. Moffett

Costa Rica Dome: Flux and Zinc Experiments

Preferential depletion of zinc within Costa Rica upwelling dome creates conditions for zinc co-limitation of primary production

P. DREUX CHAPPELL[1,2], JAGRUTI VEDMATI[3], KAREN E. SELPH[4], HEATHER A. CYR[1], BETHANY D. JENKINS[1], MICHAEL R. LANDRY[5] AND JAMES W. MOFFETT[3]*

[1]DEPARTMENT OF CELL AND MOLECULAR BIOLOGY, UNIVERSITY OF RHODE ISLAND, KINGSTON, RI 02881, USA, [2]DEPARTMENT OF OCEAN, EARTH, AND ATMOSPHERIC SCIENCES, OLD DOMINION UNIVERSITY, NORFOLK, VA 23529, USA, [3]DEPARTMENT OF BIOLOGICAL SCIENCES, UNIVERSITY OF SOUTHERN CALIFORNIA, LOS ANGELES, CA 90089, USA, [4]DEPARTMENT OF OCEANOGRAPHY, UNIVERSITY OF HAWAII AT MANOA, HONOLULU, HI 96822, USA AND [5]SCRIPPS INSTITUTION OF OCEANOGRAPHY, UNIVERSITY OF CALIFORNIA AT SAN DIEGO, 9500 GILMAN DR., LA JOLLA, CA 92093-0227, USA

*CORRESPONDING AUTHOR: jmoffett@usc.edu

The Costa Rica Dome (CRD) is a wind-driven feature characterized by high primary production and an unusual cyanobacterial bloom in surface waters. It is not clear whether this bloom arises from top-down or bottom-up processes. Several studies have argued that trace metal geochemistry within the CRD contributes to the composition of the phytoplankton assemblages, since cyanobacteria and eukaryotic phytoplankton have different transition metal requirements. Here, we report that total dissolved zinc (Zn) is significantly depleted relative to phosphate (P) and silicate (Si) within the upper water column of the CRD compared with other oceanic systems, and this may create conditions favorable for cyanobacteria, which have lower Zn requirements than their eukaryotic competitors. Shipboard grow-out experiments revealed that while Si was a limiting factor under our experimental conditions, additions of Si and either iron (Fe) or Zn led to higher biomass than Si additions alone. The addition of Fe and Zn alone did not lead to significant enhancements. Our results suggest that the depletion of Zn relative to P in upwelled waters may create conditions in the near-surface waters that favor phytoplankton with low Zn requirements, including cyanobacteria.

KEYWORDS: upwelling; zinc; phytoplankton

INTRODUCTION

The Costa Rica Dome (CRD) is characterized by persist-ent high abundance of the cyanobacterium *Synechococcus* (Saito *et al.*, 2005). Previous workers have argued that the feature might arise because the nutrient and micronu-trient regime creates conditions that favor the growth of *Synechococcus* over competitors such as diatoms (Li *et al.*, 1983; Saito *et al.*, 2005; Ahlgren *et al.*, 2014). They reported that while concentrations of nitrate (NO_3^-) and P are high, concentrations of Si and Fe are low. As a result, diatoms, which are abundant in most upwelling regimes, have a low abundance in this system.

Ahlgren *et al.* (Ahlgren *et al.*, 2014) argued that elevated cobalt (Co) concentrations in the CRD relative to outside waters contribute to high *Synechococcus* cell densities, since *Synechococcus* has a high Co requirement (Saito *et al.*, 2002, 2003, 2005) relative to eukaryotic phytoplankton (Sunda and Huntsman, 1995a; Saito *et al.*, 2002). The CRD is sustained by wind-driven upwelling of under-lying waters (Fiedler, 2002; Fiedler and Talley, 2006) from an extensive oxygen minimum zone (OMZ) that contains high concentrations of Co (Ahlgren *et al.*, 2014). Incubation studies showed that Co stimulates cyanobac-terial growth, and that Co added to incubations becomes organically complexed, possibly as part of a Co uptake mechanism (Saito *et al.*, 2005). While Co enrichment may contribute to accelerated growth of cyanobacteria, it does not account for why they predominate over eukaryotes, which normally dominate phytoplankton assemblages in upwelling regimes. For example, diatoms generally dom-inate in the Peruvian upwelling system where Co levels are also high (Saito *et al.*, 2004), and a variety of eukaryotic taxa, including *Phaeocystis*, are important in the upwelling system of the Arabian Sea (Garrison *et al.*, 1998).

Franck *et al.* (Franck *et al.*, 2003) made the observation that diatoms are co-limited by Zn and Fe in several up-welling regions, including, but not limited to, the CRD. Zn limitation has been proposed in many studies based on the high Zn requirements of diatoms and its role in the enzyme carbonic anhydrase (Morel *et al.*, 1994; Sunda and Huntsman, 1995a). Similar experiments per-formed elsewhere do not provide evidence of Zn limita-tion or co-limitation (Lohan *et al.*, 2005), yet often reveal effects on specific taxa (Crawford *et al.*, 2003; Leblanc *et al.*, 2005). Are the phenomena of Zn limitation and a persistent cyanobacterial bloom related? In order to explain the persistence of a cyanobacterial bloom, it is necessary to identify factors that would affect eukaryote growth adversely compared with cyanobacteria. Low Fe meets this criterion to a certain extent. Cyanobacteria have low growth rates and high surface area to volume ratios owing to their small size relative to other

phytoplankton. Thus, they can grow at optimal rates even when Fe is low, in spite of having similar Fe require-ments to eukaryotes (Sunda and Huntsman, 1995b). Zn limitation will have a more pronounced effect than Fe in favoring cyanobacteria over eukaryotes. In addition to the factors mentioned above, Zn requirements for cyano-bacteria are low compared with eukaryotic phytoplankton (Saito *et al.*, 2003). Surprisingly, however, there are no Zn data for the CRD reported in previous studies (Franck *et al.*, 2003; Ahlgren *et al.*, 2014).

In this study, we measured Zn profiles in the CRD during two Lagrangian experiments as part of the CRD FLUZiE (FLUx and Zinc Experiment) cruise, and we performed shipboard grow-out experiments to evaluate Zn, Fe and Si limitation and co-limitation. This work was carried out in conjunction with experimental studies of primary production, carbon cycling and trophic transfers that represent the most detailed plankton food-web study of the CRD to date (Landry *et al.*, 2016a), providing a broader biological and ecological context for these results.

METHOD

Water sampling

The FLUZiE project surveyed the CRD on R/V Melville cruise MV1008 (22 June to 25 July 2010). A series of five Lagrangian stations, designated "cycles", were carried out for 3–4 days each. The ship followed a satellite-tracked drifter with a 3 m drogue centered at 15 m as described in Landry *et al.* (Landry *et al.*, 2016a). At each cycle, a trace metal clean powder-coated rosette with 8×5 L Teflon®-coated exterior spring Niskin-type bottles (Ocean Test Equipment) was deployed using a plastic-sheathed wire, and water was collected at pre-programmed depths based on routine CTD profiles done directly pre-ceding the trace metal casts. Samples were collected between 10 and 575 m. After the rosette was brought on deck, the Niskin bottles were detached and sampled inside a clean van kept under positive pressure with HEPA-filtered air. Total dissolved metal samples were collected in acid-cleaned low-density polyethylene bottles after in-line filtration through a 0.2 μm pore-size Acropak filter using gas pressurization of the Niskin bottles with ultra-pure N_2 gas. Sampling locations are shown in Fig. 1 and Supplementary data, Table SI for each cycle, plus two transect stations (T1 and T3). Stations 11 and 13 sampled during a previous cruise to the CRD in June 2005 (KN182–5) are also shown. Note that Station 13 is in the middle of the three cycles sampled within the CRD, whereas Station 11 is much closer to the coast (outside of the CRD; Ahlgren *et al.*, 2014). Cycle 3, the
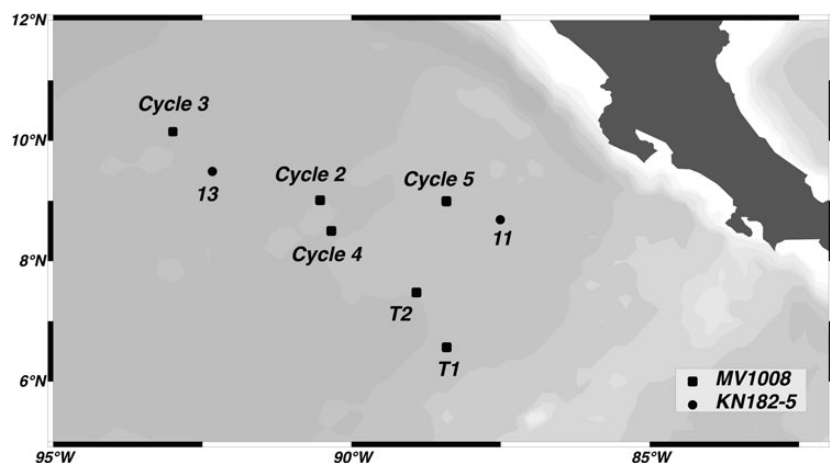
Fig. 1. Map showing the locations of all stations.

furthest offshore station, is on the western boundary of the CRD (Landry *et al.*, 2016a). Since the cycles were sampled in Lagrangian mode, locations represent the position where the trace metal sampling took place.

Metal analysis

Total dissolved Fe and Zn concentrations were determined at the University of Southern California (USC) using a single batch nitrilotriacetic acid (NTA) resin extraction and isotope dilution inductively coupled plasma mass spectrometry (ICP-MS) method adapted from Lee *et al.* (Lee *et al.*, 2011). They were analyzed in triplicate using the Finnegan Element 2 (Thermo Scientific) ICP-MS in medium resolution mode equipped with an Apex desolvation system.

Fe was pre-concentrated in the samples by adding a chelating resin—NTA Superflow resin (Qiagen) in the preparatory stage. The NTA resin was cleaned using the following procedure (Lee *et al.*, 2011): 25 mL of the NTA resin solution was poured into a clean 50 mL polypropylene centrifuge tube (Corning) and washed five times with 18.2 MΩ (Milli-Q) water. Between washes, the tube was spun down in a 5810-R centrifuge (Eppendorf) maintained at 8°C for 10 min at 3220 × g. After decanting the supernatant, Milli-Q water was added for the next wash. The resin was then washed five times with 1.5 M trace metal grade hydrochloric acid (HCl; Optima, Fisher) and several more times with Milli-Q water after that to bring the pH of the solution above 4, indicating that all of the HCl had been removed from the solution. For the final cleaning step, the resin solution was washed five times with 0.5 M trace metal grade nitric acid (HNO₃; Optima, Fisher). The resin solution was placed on an analog shaker for several hours for the first wash

and then left overnight on the shaker for the last wash. After the final wash, the resin solution was again washed at least five times with Milli-Q water until the pH had risen above 4 in order to remove all of the HNO₃. The resin solution was diluted two-fold with 25 mL Milli-Q water and stored in the refrigerator for future use. A 25 μL working volume of the resin suspension contained ∼100–400 beads, representing a 1:50 dilution of the primary resin solution.

Samples were pre-concentrated for analysis in 15 mL polypropylene centrifuge tubes, which were first cleaned in a two-step process by soaking them in 10% HCl at 60°C for 48 h and then rinsing each tube at least five times with Milli-Q water. After the rinses, the tubes were filled to a positive meniscus with 0.5% trace metal grade HCl, capped and baked at 60°C overnight. After retrieving them from the oven, the tubes were left capped and stored until used. Before sample addition, the tubes were emptied and rinsed three times with Milli-Q water and at least once with the sample.

The centrifuge tubes were filled with ∼7.5 mL of sample (with the exact volume determined gravimetrically) and spiked with enough ^{57}Fe-enriched spike and ^{67}Zn-enriched spike (BDH Aristar Plus) to bring the final concentration to ∼2 nM. Subsequently, 0.1 mL of 1.5 M trace metal grade hydrogen peroxide (Optima, Fisher) was added to each sample and left to equilibrate for at least an hour at room temperature, to completely oxidize any Fe(II) to Fe(III) (Lee *et al.*, 2011). Next, 200 μL (∼800 beads) of the working resin suspension was added to each sample, and the tubes were placed on a shaker for 2–3 days. The samples were centrifuged for 10 min at 3220 × g, and the seawater was siphoned off to leave the resin beads. The beads were washed twice with 3 mL Milli-Q water to remove salts and the tubes were once

again centrifuged using the same settings. After the final wash, 1 mL of 5% trace metal grade HNO_3 was added to each tube and, after leaving them on the shaker again for 1 day, the samples were ready for analysis.

Procedural seawater blanks were prepared in triplicate in the same way as samples using ∼0.2 mL low trace metal surface seawater from the 2004 Sampling and Analysis of Iron (SAFe) cruise (DFe = 0.09 ± 0.007 nmol L^{-1}). The average detection limit and internal blank value for this method ($n = 3$, 1σ) for Fe were 0.01 and 0.06 nM, respectively. The accuracy of the method was evaluated by measuring SAFe reference standards S1 and D1 (Johnson *et al.*, 2007). The Fe values we obtained by this method for S1 and D1 were 0.094 ± 0.01 and 0.645 ± 0.02 nM, respectively. The latest consensus values are 0.093 ± 0.008 nM Fe (S1) and 0.67 ± 0.04 nM Fe (D1) (http://www.geotraces.org/science/intercalibration).

Nutrient analysis

Nutrient samples from samples shallower than 100 m were analyzed for soluble reactive P and Si concentration by flow injection analysis at the nutrient laboratory of the University of California, Santa Barbara on a Lachat Instruments QuikChem 8000 using standard wet-chemistry methods (Gordon *et al.*, 1992). All NO_3^- measurements and P data from samples collected deeper than 100 m were made using a WestCo SmartChem 200 discrete analyzer in the Stanford University Environmental Measurement 1: Gas-Solution Analytical Center and are also presented elsewhere (Buchwald *et al.*, 2015).

Incubation setup

Deck-board incubations were set up using water collected shortly after dawn from the base of the mixed layer using the trace metal sampling rosette at Cycles 2−4 (Fig. 1; Landry *et al.*, 2016a). The incubation setup was done in the clean van. All acid-cleaned 2 L Nalgene® polycarbonate incubation bottles were rinsed at least two times with sample water and then filled using an acid-cleaned piece of bev-a-line tubing to transfer the water from the Niskin bottle to the polycarbonate incubation bottles. Nutrient treatments were as follows: Control (no additions); +2 nM Zn (added as zinc chloride); +5 nM Fe (added as ferric chloride); +2 μM Si (added as sodium silicate); +2 nM Zn +2 μM Si (Cycles 3 and 4 only); +5 nM Fe +2 μM Si (Cycle 4 only). The levels for nutrient additions were chosen based on previous studies from the region (Franck *et al.*, 2003; Saito *et al.*, 2005) as values that should be high enough to be replete, but not so high that they would cause a toxic effect. Following nutrient amendment additions, incubation bottles were placed inside Plexiglas incubators with a blue plastic coating (Rosco: Saito *et al.*, 2005) with circulating surface ocean water that were fastened to the back deck for a period of 72 h.

Incubation sampling

At the end of the incubation, unfiltered samples were collected for shipboard and shore-based flow cytometry (FCM). Shipboard samples were kept on ice in the dark until analysis (within 1−2 h) without preservation. The shipboard flow cytometer was a Beckman-Coulter EPICS XL with a 15 mW, 488 nm argon ion laser with an Orion syringe pump that delivered 2.2 mL samples at a rate of 0.44 mL min^{-1}. Listmode data files (FCS 2.0 format) of cell fluorescence and light-scatter properties were acquired with Expo32 software and analyzed with FlowJo software. Fluorescence signals were normalized to 6.0 μm yellow−green (YG) polystyrene beads (Polysciences Inc., Warrington, PA, USA). Normalized forward light scatter was calibrated relative to known diameters of fluorescent YG beads to derive rough size classes of photosynthetic eukaryotes in each sample (<2 μm, pico; 2−20 μm, nano; >20 μm, micro). Because the shipboard flow cytometer is not sensitive enough to detect *Prochlorococcus*, shore-based analyses were done for this population. Samples (2 mL) were preserved (0.5% paraformaldehyde, v/v, final concentration) and frozen in liquid nitrogen on shipboard, and stored at −80°C until analysis. In the laboratory after the cruise, the samples were thawed and stained with Hoechst 33342 (1 μg mL^{-1}, v/v, final concentration) at room temperature in the dark for 1 h (Monger and Landry, 1993). Aliquots (100 μL) were analyzed using a Beckman-Coulter EPICS Altra flow cytometer with a Harvard Apparatus syringe pump for volumetric sample delivery. Simultaneous (co-linear) excitation of the plankton was provided by two water-cooled 5 W argon ion lasers, tuned to 488 nm (1 W) and the UV range (200 mW). The optical filter configuration distinguished populations on the basis of chlorophyll *a* (red fluorescence, 680 nm), phycoerythrin (orange fluorescence, 575 nm), DNA (blue fluorescence, 450 nm) and forward and 90° side scatter signatures. Calibration beads (0.5 and 1.0 μm YG beads and 0.5 μm UV beads) were used as fluorescence standards. Raw data (listmode files) were processed using the software FlowJo (Treestar Inc., www.flowjo.com).

Additionally, samples were filtered onto a glass fiber filter (GF/F) using a vacuum pump for chlorophyll analysis using standard techniques (Herbland *et al.*, 1985).

Statistical analysis

All statistical analyses were done using Matlab software version R2013B. Statistical analyses consisted of analysis

of variance (ANOVA) with a Tukey HSD *post hoc* test on Chl *a* data for all treatments in individual incubations. FCM data were treated similarly, where counts for each group (*Synechococcus*, *Prochlorococcus* and photosynthetic eukaryotes broken down into pico-, nano- and micro-size classes) were analyzed against counts for that same group across different treatments within a single incubation.

RESULTS

Water column nutrients and trace metals

Fe and Zn exhibited nutrient-like features in Cycles 3 and 4, with exceedingly low concentrations in surface waters (Figs 2 and 3 and Tables I–IV). Upper water column data from other locations (Table V) indicate that low Fe and Zn in the upper water column is a characteristic feature of the region. Zn and Fe data for two stations sampled in 2005 on KN182-5 show that these overall trends are consistent over time (Tables VI and VII).

Fe concentrations increased between 30 and 100 m in Cycles 3 and 4, forming local maxima ∼80 m, although Fe was still exceedingly low through this depth range. Fe concentrations show a pronounced increase ∼400 m.

Incubation results

Bulk Chlorophyll a *responses to nutrient and trace metal additions*

The addition of Zn or Fe alone had no significant effect on Chl *a* concentrations relative to the control at any cycle (Fig. 4). The addition of Si alone resulted in an increase in Chl *a*, which was significant in Cycle 2 incubations, but the co-additions of Zn + Si and Fe + Si had the largest effects ($P < 0.05$, ANOVA) in Cycles 3 and 4. Interestingly, Chl *a* was lower in the Zn only treatments than in the control samples in Cycles 2 and 3, although this difference was not significant.

Different phytoplankton group responses to nutrient and trace metal additions

FCM results for the photosynthetic eukaryotes (divided into pico-, nano- and micro-size classes using relative forward light scatter signals) were relatively consistent across both Cycles 3 and 4 incubations (Fig. 5, Supplementary data, Tables SII and SIII). In Cycle 3 (Fig. 5A, Supplementary data, Table SII), Zn + Si co-addition led to a significant increase in the abundance of photosynthetic eukaryotes of the nano- and micro-size classes when compared with Fe addition treatments ($P < 0.05$, ANOVA). Zn + Si co-addition also led to a significant increase in the abundance of micro-size photosynthetic eukaryotes when compared with Zn addition treatments ($P < 0.05$, ANOVA). In Cycle 4 (Fig. 5B, Supplementary data, Table SIII), the FCM for photosynthetic eukaryotes in the pico- and micro-size classes showed significantly higher ($P < 0.05$, ANOVA) counts in the Zn + Si co-addition treatment when compared with all treatments except the Fe + Si co-addition treatment.

The results for the two groups of cyanobacteria differed in the two incubations (Fig. 5, Supplementary data, Tables SII and SIII). In Cycle 3, Zn + Si co-addition had a
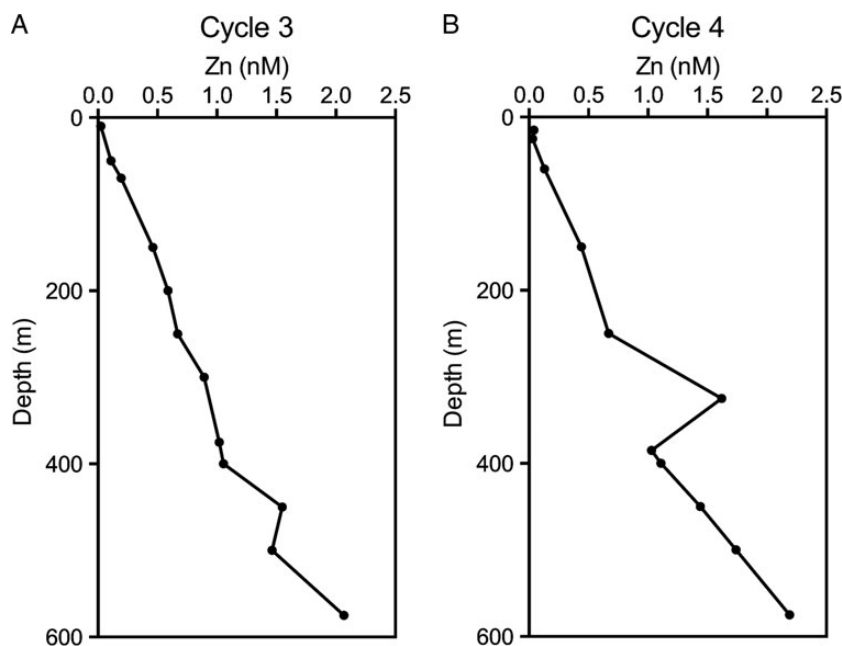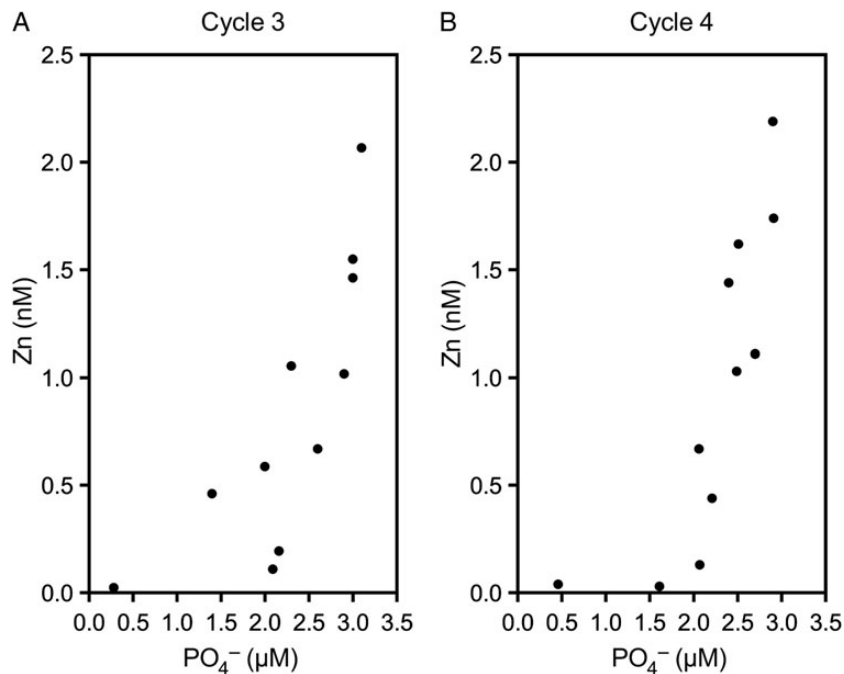

Fig. 2. Plots of dissolved Zn versus depth at (**A**) Cycle 3 and (**B**) Cycle 4.

Fig. 3. (**A**) Plot of Zn versus P for Cycle 3. (**B**) Plot of Zn versus P for Cycle 4.

Table I: Dissolved Fe and Zn Concentration for Cycle 3

Depth (m)	Zn (nM)	Zn Stdev (nM)	Fe (nM)	Fe Stdev (nM)
10	0.024	0.018	0.044	0.002
20			0.062	0.000
30			0.134	0.005
50	0.110	0.003	0.267	0.003
70	0.195	0.001	0.524	0.007
100			0.657	0.041
150	0.461	0.002	0.663	0.009
175			0.610	0.002
200	0.588	0.002	0.637	0.023
250	0.670	0.010	0.684	0.005
300	0.892	0.007	0.800	0.004
375	1.019	0.004	0.940	0.000
390			1.082	0.005
400	1.055	0.007	1.059	0.004
425			1.073	0.041
450	1.549	0.004	1.272	0.001
475			1.085	0.011
480			1.402	0.016
500	1.463	0.004	1.424	0.004
550			1.356	0.011
575	2.067	0.035	1.450	0.023

Stdev represents the standard deviation of analytical variability of triplicate measurements.

Table II: Dissolved Fe and Zn concentrations for Cycle 4

Depth (m)	Zn (nM)	Zn Stdev (nM)	Fe (nM)	Fe Stdev (nM)
15	0.04	0.00	0.016	0.004
20			0.026	0.001
25	0.03	0.01	0.045	0.005
35			0.082	0.001
60	0.13	0.01	0.220	0.005
100			0.394	0.003
150	0.44	0.00	0.525	0.002
175			0.397	0.002
200			0.551	0.009
250	0.67	0.00	0.579	0.001
300			0.582	0.007
325	1.62	0.02	1.250	0.007
385	1.03	0.04	1.355	0.026
400	1.11	0.00	1.362	0.001
415			1.315	0.004
425			1.300	0.050
450	1.44	0.02	1.394	0.001
475			1.082	0.003
500	1.74	0.01	1.175	0.007
550			0.932	0.004
575	2.19	0.02	1.201	0.006

Stdev represents the standard deviation of analytical variability of triplicate measurements.

significant positive effect on *Prochlorococcus* abundances compared with control treatments ($P < 0.05$, ANOVA). Zn addition also had a significant negative effect on *Prochlorococcus* ($P < 0.05$, ANOVA) when compared with Si or Zn + Si

co-addition treatments. In Cycle 4, the FCM data show that *Synechococcus* abundances were significantly higher in the single addition Si treatment when compared with the Zn + Si co-addition treatment ($P < 0.05$, ANOVA).

Table III: Nutrient concentrations for Cycle 3

Depth (m)	NO_3^- (μM)	P (μM)	Si (μM)
3	0.61	0.24	1.77
15	1.57	0.28	1.74
20	4.87	0.69	4.03
25	11.4	2.20	
30	25.5	1.82	13.46
40	26.0	2.09	19.55
60	14.9	2.16	21.37
83	27.8	2.20	22.64
97	32.9	2.27	24.43
152	25.1	1.40	
198	19.9	2.00	
250	35.4	2.60	
300	17.6		
350	16.8	2.90	
400	17.5	2.30	
450	29.8	3.00	
500	31.1	3.00	
550	33.8	3.20	
600	38.7	3.10	

Note that Si was not measured below 100 m.

Table IV: Nutrient concentrations for Cycle 4

Depth (m)	NO_3^- (μM)	P (μM)	Si (μM)
2	1.61	0.28	3.01
15	6.30	0.46	3.99
20	11.4	1.70	12.83
25	24.9	1.61	
30	51.1	2.04	18.46
40	16.8	2.22	21.24
61	22.6	2.07	21.44
81	15.9	2.23	22.96
100	13.2	1.84	
198	14.1	2.21	
300	47.4	2.06	
350	22.1	2.51	
375	29.4	2.49	
402	29.7	2.70	
425	27.6	2.93	
451	27.3	2.40	
475	23.3	2.87	
503	20.2	2.91	
603	25.8	2.90	

Note that Si was not measured below 100 m.

DISCUSSION

Zn is substantially depleted relative to P and Si in the upper 200 m of the water column. While both P and Si increase dramatically between 30 and 100 m below the mixed layer at all stations, Zn increases only slightly. This does not mean that Zn is decoupled from nutrients throughout the water column. The data plotted in Fig. 3 show a linear relationship with P in the upper 500 m, a feature that is characteristic of other regions, including the North Pacific (Lohan *et al.*, 2005; Jakuba *et al.*, 2012). Note that the change in slope below 1 μM P is also

Table V: Near-surface Zn and Fe data for selected stations MV1008

Station	Depth (m)	Zn (nM)	Zn Stdev (nM)	Fe (nM)	Fe Stdev (nM)
Cycle 2	12	0.078	0.002	0.089	0.01
	40	0.076	0.007	0.061	0.003
Cycle 5	12	0.079	0.013	0.055	0.030
	40	0.127	0.003	0.376*	0.011
T1	15	0.032	0.002	No data	
	30	0.017	0.003		
T3	15	0.078	0.002	No data	
	45	0.186	0.014		

Stdev represents the standard deviation of analytical variability of triplicate measurements.
*Contamination suspected.

Table VI: P, Si, Zn and Fe data from Sta. 11 KN182-5

Depth (m)	P (μM)	Si (μM)	Avg. Fe (nM)	Fe Stdev (nM)	Avg. Zn (nM)	Fe Stdev (nM)
13	0.2	1.5	0.08	0.01	0.50	0.03
55	1.3	14.5	0.13	0.00	0.53	0.03
99			0.06	0.00	0.59	0.10
270	2.3	28.3	0.95	0.02	0.81	0.04
320			1.04	0.02	0.96	0.01
380	1.9	30	1.27	0.02	1.42	0.01
400	2.8	43.7	0.57	0.01	0.49	0.04
500	2.9	51.9	1.16	0.01	1.80	0.05
550			0.69	0.02	1.16	0.08
703	3.6	72	1.12	0.02	3.47	0.03
800			1.05	0.06	3.86	0.09
931	3.2	74.6	1.19	0.01	4.56	0.35

Stdev represents the standard deviation of analytical variability of triplicate measurements.

reported in those studies where it is attributed to P drawdown under oligotrophic conditions by taxa that have a low Zn requirement (Sunda and Huntsman, 1995a). A comparison of data from the North Pacific with data from this study (Fig. 6) indicates that Zn is substantially depleted relative to P in waters underlying the CRD. Therefore, upwelling in the CRD supplies water that is enriched in P, but depleted in Zn.

Worldwide, while Zn and P have a linear relationship shallower than 1000 m, this correlation breaks down in deep waters, where Zn retains a strong correlation with Si (Schlitzer, 2000). It is key to determine how important the processes associated with the preferential removal of Si might be for Zn. Data from the KN182-5 cruise, which was sampled for both Si and P down to 1000 m, and data from the surface to 100 m from the 2010 cruise show a linear relationship between Si and P between 20 and 200 m, with a slope of ∼10 (representative data from Stn 11 shown in Table VI), compared with a slope of ∼13−20 in the stations where Zn data are shown in

Fig. 6, as reported in Jakuba *et al.* (Jakuba *et al.*, 2012). This is consistent with the efficient Si export mechanism observed on the cruise (Krause *et al.*, 2016) and could

Table VII: *Zn and Fe data from Sta. 13 KN182-5*

Depth (m)	Avg. Fe (nM)	Fe Stdev (nM)	Avg. Zn (nM)	Zn Stdev (nM)
80	0.08	0.01	0.28	0.02
266	0.57	0.01	0.88	0.01
375	1.00	0.02	1.24	0.09
500	1.07	0.00	1.79	0.02
650	0.95	0.02	2.79	0.04

Stdev represents the standard deviation of analytical variability of triplicate measurements.
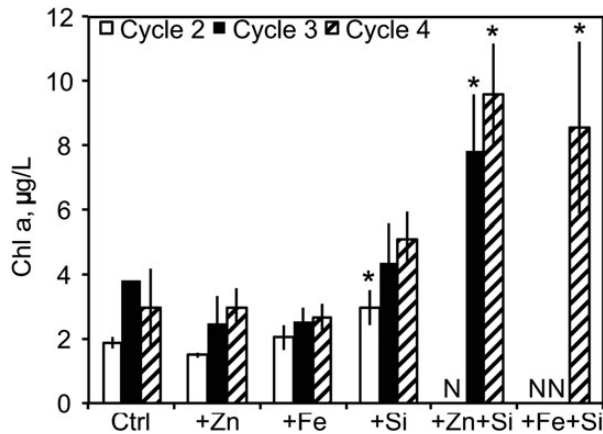
Fig. 4. Chl *a* (μg L^{-1}) measured from samples taken from biological triplicate incubation bottles for each treatment from all three cycles. *Value is statistically larger than control treatment, single addition zinc treatment and single addition iron treatment for that cycle ($P < 0.05$, ANOVA). "N" indicates that a treatment was not performed at that cycle.
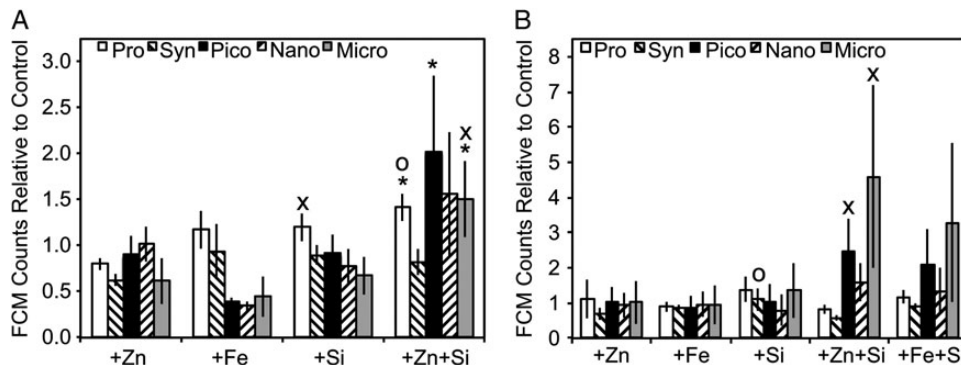
point to a contribution to Zn depletion by a process that also preferentially removes Si, perhaps export of diatoms or other taxa enriched in both elements. Therefore, much of the difference between Zn at the CRD and North Pacific could reflect the differing behavior of Si in each region.

We hypothesize that Zn depletion relative to P, coupled with the shallow stratification within the CRD sets up a cycle where waters with low Zn:P ratios are upwelled, leading to growth of phytoplankton with low Zn requirements. As a result, Zn:P in exported organic matter is low, reinforcing the cycle. That mechanism is supported by Baines *et al.* (Baines *et al.*, 2016) who reported some of the lowest Zn:C ratios ever reported in the smallest plankton size class. Figure 7 illustrates how these various factors may interact to perpetuate a low Zn cycle. Any episodic inputs of waters containing elevated Zn, which would also be elevated in Si and P, leads to diatom growth, which is exported to depth. At other times, the supply of micronutrients to taxa with low Zn requirements must be adequate to maintain a significant biological pump transporting Zn-depleted organic matter out of the euphotic zone and into the underlying waters. This component of the process is where the elevated Co supply outlined in Ahlgren *et al.* (Ahlgren *et al.*, 2014) becomes very important, since taxa with low Zn requirements often have high Co requirements (Sunda and Huntsman, 1995a).

What makes the CRD different than the North Pacific, where Zn:P ratios are higher (Fig. 6)? One possibility is that in the CRD, the absence of deep winter mixing means fewer episodic injections of waters enriched with Zn into the euphotic zone compared with the temperate N Pacific. Hence the shallow pycnocline of the CRD is a

Fig. 5. (**A**) FCM counts relative to control treatment for Cycle 3 incubation measured in biological triplicates. *Counts for this size class were statistically higher than those of the single addition Fe treatments. o indicates that counts for this size class were statistically higher than those in single addition control treatment. *x* indicates that counts for that size class were statistically higher than those of the single addition Zn treatment ($P < 0.05$, ANOVA). Syn, *Synechococcus*; Pro, *Prochlorococcus*; PicoEuk, NanoEuk and MicroEuk, photosynthetic eukaryotic phytoplankton in three size classes, as defined in the text. (**B**) FCM counts relative to control treatment for Cycle 4 incubation measured in biological triplicates. *x* indicates the counts for this size class were statistically higher than those in all other treatments but +Si + Fe. o indicates that the counts for this size class were statistically higher than those in the +Zn + Si co-addition treatment ($P < 0.05$, ANOVA). Abbreviations as above.

critical feature. Another possibility is that the export of organic matter derived from phytoplankton with higher Zn:P ratios may be more efficient than organic matter derived from picoplankton with low Zn:P ratios. This is consistent with the findings of Krause et al. (Krause et al., 2016), who studied Si uptake and regeneration on the FLUZiE cruise. They concluded that there is a high efficiency Si pump within the CRD that is presumably driven by production of diatoms, which have a high Zn requirement.

A shortcoming of this scenario is that it does not account for the decoupling of Zn from both Si and P in the upper 100 m. Dissolved Zn:Si ratios remain low between 30 and 100 m (where Si is higher than in

Fig. 6. Zn vs. P in the North Pacific Ocean (Jakuba et al., 2012) and CRD.

surface waters but Zn is not), suggesting that if there is an efficient Si pump, the "Zn pump" must be even more efficient. We argue below that there is probably an additional removal process, associated with scavenging. One possible explanation is that the release of Zn during remineralization of sinking organic matter is impeded under the reducing conditions prevailing within the OMZ below the CRD. Janssen et al. (Janssen et al., 2014) have argued that Cd is preferentially removed by sulfide within OMZs, possibly in anoxic microenvironments within sinking particles. Sequestration of Zn by reduced sulfur on settling particles might also be important. Canfield et al. (Canfield et al., 2010) argued that "cryptic" sulfate reduction occurs within particles in OMZs, providing a source of sulfide for this process. Sulfate reduction and sulfide formation in microenvironments could be important in the water column where oxygen is low but not necessarily absent, which was the case in some of the areas observed in Janssen et al. (Janssen et al., 2014). Thus, in situ scavenging by this mechanism could be important within the source of upwelled waters even though oxygen disappears at a much greater depth. A mechanism for Zn scavenging onto sinking particles is also necessary; because it is unlikely that grazing and fecal pellet production alone could supply a Zn pump. While mesozooplankton have high assimilation and regeneration efficiencies for Zn, only a small fraction of this Zn is incorporated into sinking particles (Wang et al., 1996).

Recent models of Zn and Zn isotope distributions suggest that Zn scavenging is widespread, even in oxic conditions (John and Conway, 2014). Thus, our findings
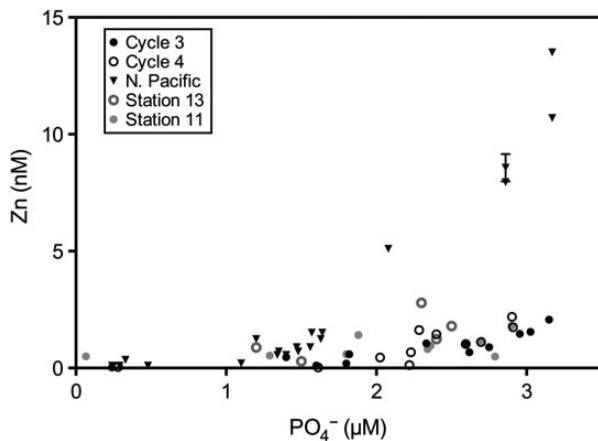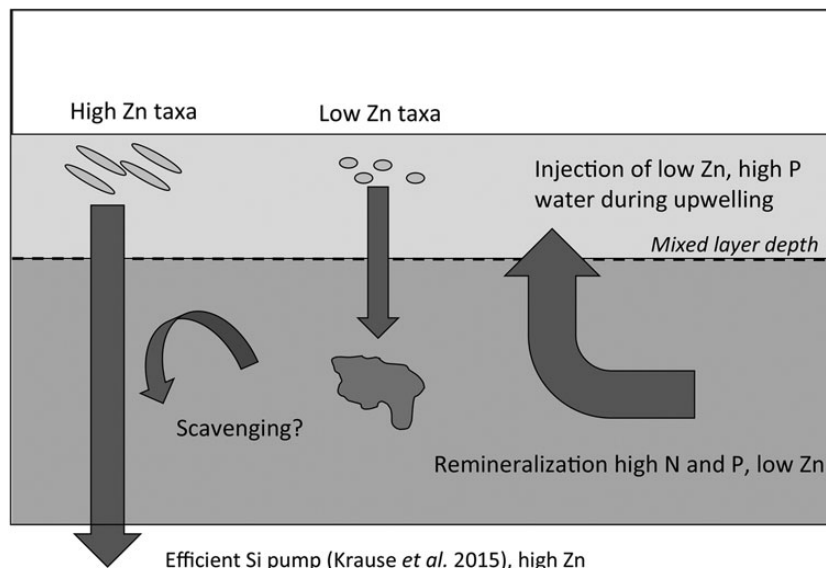

Fig. 7. Conceptual diagram of processes contributing to Zn depletion within the CRD. Note that export below the box is lost to the upwelling cycle. "High Zn taxa" include diatoms; "low Zn taxa" include cyanobacteria.

may not be unique to the CRD, but may point to Zn scavenging being more pronounced in waters with an oxygen deficit. The difference could arise from the presence of reduced sulfur as described above or perhaps be the result of another distinct aspect of sinking particle chemistry in low oxygen waters.

Note that the distinct feature of the Zn distribution over the CRD is not the low surface concentrations. Similar low surface values have been reported in the North Pacific (Bruland, 1980; Lohan *et al.*, 2002; Jakuba *et al.*, 2012), subtropical North Atlantic (Jakuba *et al.*, 2008; Conway and John, 2014) and the California Coastal upwelling (Franck *et al.*, 2003). The key feature is that the ratio of Zn to P is lower in the subsurface waters (where P ranges from 1 to 2 μM), so that upwelled water does not replenish Zn supply.

Fe is also low in surface waters, and the values are comparable to Fe concentrations in many HNLC areas. Surface Fe in the CRD in this study is similar to concentrations in the CRD in 2000 reported by Franck *et al.* (Franck *et al.*, 2003) and in 2005 reported by Ahlgren *et al.* (Ahlgren *et al.*, 2014). Thus, it appears that persistent Fe limitation is a characteristic feature of the CRD. This may seem surprising, since there is a subsurface maximum in Fe associated with an Fe(II) feature in the underlying secondary nitrite maximum. However, this feature is much deeper in the CRD than in other OMZs, at $\sim$350 m (Vedamati, 2013). A small local maxima in Fe $\sim$80−100 m, although modest and much smaller than Fe increases at greater depth, suggests that upwelled water is more enriched in Fe than it is in Zn. In contrast, elevated Co concentrations persist well above the oxic/anoxic interface (Ahlgren *et al.*, 2014) and so upwelling waters do supply high Co. This could reflect the differing redox dynamics, as Co(II) oxidation kinetics are much slower than Fe(II) (Moffett and Ho, 1996).

The bulk Chl *a* incubation results indicate that both Si and trace metal availability (either Zn or Fe) co-limit primary productivity in the surface mixed layer. FCM allowed us to delve further into the responses of individual components of the phytoplankton community to the various nutrient additions. In the two incubations with FCM data, there was a significant response in the eukaryotic algal community, presumably diatoms (given their Si requirement), to Zn + Si co-addition. Si concentrations in the mixed layer were not zero at the start of the incubation, so why would these organisms not be stimulated by Zn additions alone? Previous studies of trace metal controls on Si and NO_3^- uptake in the CRD have found that Zn addition led to an increase in Si uptake relative to NO_3^- uptake (Franck *et al.*, 2003). It is therefore possible that an increase in the Si:NO_3^- uptake by diatoms in

response to Zn addition without Si addition would quickly deplete the remaining Si in the water. This could lead to a boom and bust of diatoms over the course of our 72 h incubations. If we had sampled earlier in the incubation, we may have seen a response to Zn addition alone. Higher *Synechococcus* abundances in the +Si treatment when compared with abundances in the Zn + Si co-addition treatment in Cycle 4 could reflect *Synechococcus* being out-competed for nutrients by diatoms in the Zn + Si co-addition treatment. This mechanism cannot explain why *Prochlorococcus* abundances responded positively to Zn + Si co-addition treatment at Cycle 3, which was at the edge of the CRD core. It is possible that a high ratio of Si:NO_3^- drawdown by the diatoms somehow opened a niche for *Prochlorococcus*, but the exact mechanism to explain this remains unclear. That the significant *Prochlorococcus* response was only seen in Cycle 3 incubation and the significant *Synechococcus* response was only seen in Cycle 4 incubation suggests that the effects of trace metals on cyanobacterial growth vary across the region. In contrast, the consistent positive response to Zn + Si co-addition in the eukaryotic size classes suggests that Zn−Si co-limitation of the diatom community is pervasive across the CRD. This finding is generally consistent with other taxa-specific studies of response to Zn additions, even in places where the role of Zn in regulating primary production is slight (Crawford *et al.*, 2003; Leblanc *et al.*, 2005).

The results suggest that low Zn concentrations influence the composition of phytoplankton assemblages in this region. Indeed, diatoms, taxa with a high Zn requirement, constituted only $\sim$3% of the primary production with the CRD during our study (Selph *et al.*, 2016). Landry *et al.* (Landry *et al.*, 2016b) concluded that primary production is not controlled by grazing, especially for the larger eukaryotic taxa that are likely to rely on Zn (Sunda and Huntsman, 1995a). This suggests that bottom-up control is regulating the growth of these taxa, presumably involving Si and Zn. Our results are also consistent with the low Zn:C ratios of Baines *et al.* (Baines *et al.*, 2016). Moreover, those workers found Si within all size classes, including the prokaryotes, which could account for the evidence of Si co-limitation we observed. Zn could be particularly important in regions where it is depleted relative to nutrients and Zn resupply is constrained by factors noted above. Perhaps large areas of the eastern tropical Pacific share these characteristics. While Zn limitation studies have not been performed in these areas, we do know that the phenomenon of a cyanobacterial surface bloom is unusual. That suggests that the interplay of a whole suite of factors, including Fe limitation and abundant Co, contribute to the phytoplankton community structure at this site.

REFERENCES

Ahlgren, N. A., Noble, A., Patton, A. P., Roache-Johnson, K., Jackson, L., Robinson, D., McKay, C., Moore, L. R. *et al.* (2014) The unique trace metal and mixed layer conditions of the Costa Rica upwelling dome support a distinct and dense community of *Synechococcus*. *Limnol. Oceanogr.*, **59**, 2166–2184.

Baines, S. B., Vogt, S., Chen, X., Twining, B. S. and Landry, M. R. (2016) Elemental content of phytoplankton in the Costa Rica Upwelling Dome and mineral limitation of mesozooplankton production. *J. Plankton Res.*, **38**, 256–270.

Bruland, K. W. (1980) Oceanographic distributions of cadmium, zinc, nickel, and copper in the North Pacific. *Earth Planet. Sci. Lett.*, **47**, 176–198.

Buchwald, C., Santoro, A. E., Stanley, R. H. R. and Casciotti, K. L. (2015) Nitrogen cycling in the secondary nitrite maximum in the Costa Rica Upwelling Dome. *Global Biogeochem. Cycles*, **29**, doi:10.1002/2015GB005187.

Canfield, D. E., Stewart, F., Thamdrup, B., De Brabandere, L., Dalsgaard, T., Delong, E. F., Revsbech, N. P. and Ulloa, O. (2010) A cryptic sulfur cycle in oxygen-minimum-zone waters off the Chilean Coast. *Science*, **330**, 1375–1378.

Conway, T. M. and John, S. G. (2014) The biogeochemical cycling of zinc and zinc isotopes in the North Atlantic Ocean. *Global Biogeochem. Cycles*, **28**, 1111–1128.

Crawford, D. W., Lipsen, M. S., Purdie, D. A., Lohan, M. C., Statham, P. J., Whitney, F. A., Putland, J. N., Johnson, W. K. *et al.* (2003) Influence of zinc and iron enrichments on phytoplankton growth in the Northeastern subarctic Pacific. *Limnol. Oceanogr.*, **48**, 1583–1600.

Fiedler, P. C. (2002) The annual cycle and biological effects of the Costa Rica Dome. *Deep-Sea Res. Part I*, **49**, 321–338.

Fiedler, P. C. and Talley, L. D. (2006) Hydrography of the eastern tropical Pacific: a review. *Prog. Oceanogr.*, **69**, 143–180.

Franck, V. M., Bruland, K. W., Hutchins, D. A. and Brzezinski, M. A. (2003) Iron and zinc effects on silicic acid and nitrate uptake kinetics in three high-nutrient, low-chlorophyll (HNLC) regions. *Mar. Ecol. Prog. Ser.*, **252**, 15–33.

Garrison, D. L., Gowing, M. M. and Hughes, M. P. (1998) Nano- and microplankton in the northern Arabian Sea during the Southwest Monsoon August-September, 1995: a U.S. JGOFS study. *Deep-Sea Res. Part II*, **45**, 2269–2299.

Gordon, L. I., Jennings, J. C., Ross, A. A. and Krest, J. M. (1992) A suggested protocol for continuous flow automated analysis of seawater nutrients in the WOCE hydrographic program and the Joint Global Ocean Fluxes Study. Grp. Tech Rpt, Chemical Oceanography Group OSU College of Oceanography, 92-1.

Herbland, A., Lebouteiller, A. and Raimbault, P. (1985) Size structure of phytoplankton biomass in the equatorial Atlantic-Ocean. *Deep-Sea Res., Part A*, **32**, 819–836.

Jakuba, R. W., Moffett, J. W. and Dyrhman, S. (2008) Evidence for the linked biogeochemical cycling of zinc, cobalt, and phosphorus in the western North Atlantic Ocean. *Global Biogeochem. Cycles*, **22**, GB4012.

Jakuba, R. W., Saito, M. A., Moffett, J. W. and Xu, Y. (2012) Dissolved zinc in the subarctic North Pacific and Bering Sea: its distribution, speciation, and importance to primary producers. *Global Biogeochem. Cycles*, **26**, doi:10.1029/2010GB004004.

Janssen, D. J., Conway, T. M., John, S. G., Christian, J. R., Kramer, D. I., Pedersen, T. F. and Cullen, J. T. (2014) Undocumented water column sink for cadmium in open ocean oxygen-deficient zones. *Proc. Natl Acad. Sci. USA*, **111**, 6888–6893.

John, S. G. and Conway, T. M. (2014) A role for scavenging in the marine biogeochemical cycling of zinc and zinc isotopes. *Earth Planet. Sci. Lett.*, **394**, 159–167.

Johnson, K. S., Elrod, V., Fitzwater, S., Plant, J., Boyle, E., Bergquist, B., Bruland, K., Aguilar-Islas, A. *et al.* (2007) Developing standards for dissolved iron in seawater. *EOS Trans. AGU*, **88**, 131–132.

Krause, J., Stukel, M. R., Taylor, A. G., Taniguchi, D. A., de Verneil, A. and Landry, M. R. (2016) Net biogenic silica production and the contribution of diatoms to new production and organic matter export in the Costa Rica Dome ecosystem. *J. Plankton Res.*, **38**, 216–229.

Landry, M. R., de Verneil, A., Goes, J. and Moffett, J. W. (2016a) Plankton dynamics and biogeochemical fluxes in the Costa Rica Dome: introduction to the CRD Flux and Zinc Experiments. *J. Plankton Res.*, **38**, 167–182.

Landry, M. R., Selph, K. E., Décima, M., Gutiérrez-Rodríguez, A., Stukel, M. R., Taylor, A. G. and Pasulka, A. L. (2016b) Phytoplankton production and grazing balances in the Costa Rica Dome. *J. Plankton Res.*, **38**, 366–379.

Leblanc, K., Hare, C. E., Boyd, P. W., Bruland, K. W., Sohst, B., Pickmere, S., Lohan, M. C., Buck, K. *et al.* (2005) Fe and Zn effects on the SiO_4^{2-}-cycle and diatom community structure in two contrasting high and low-silicate HNLC areas. *Deep Sea Res. Part I*, **52**, 1842–1864.

Lee, J. M., Boyle, E. A., Echegoyen-Sanz, Y., Fitzsimmons, J. N., Zhang, R. F. and Kayser, R. A. (2011) Analysis of trace metals (Cu, Cd, Pb, and Fe) in seawater using single batch nitrilotriacetate resin extraction and isotope dilution inductively coupled plasma mass spectrometry. *Anal. Chim. Acta*, **686**, 93–101.

Li, W. K. W., Rao, D. V. S., Harrison, W. G., Smith, J. C., Cullen, J. J., Irwin, B. and Platt, T. (1983) Autotrophic picoplankton in the tropical ocean. *Science*, **219**, 292–295.

Lohan, M. C., Statham, P. J. and Crawford, D. W. (2002) Total dissolved zinc in the upper water column of the subarctic North East Pacific. *Deep Sea Res. Part II*, **49**, 5793–5808.

Lohan, M. C., Crawford, D. W., Purdie, D. A. and Statham, P. J. (2005) Iron and zinc enrichments in the northeastern subarctic

Pacific: ligand production and zinc availability in response to phytoplankton growth. *Limnol. Oceanogr.*, **50**, 1427–1437.

Moffett, J. W. and Ho, J. (1996) Oxidation of cobalt and manganese in seawater via a common microbially catalyzed pathway. *Geochim. Cosmochim. Acta*, **60**, 3415–3424.

Monger, B. C. and Landry, M. R. (1993) Flow cytometric analysis of marine bacteria with Hoechst 33342. *Appl. Environ. Microbiol.*, **59**, 905–911.

Morel, F. M. M., Reinfelder, J. R., Roberts, S. B., Chamerlain, C. P., Lee, J. G. and Yee, D. (1994) Zinc and carbon co-limitation of marine phytoplankton. *Nature*, **369**, 740–742.

Saito, M. A., Moffett, J. W., Chisholm, S. W. and Waterbury, J. W. (2002) Cobalt limitation and uptake in *Prochlorococcus*. *Limnol. Oceanogr.*, **47**, 1629–1636.

Saito, M., Sigman, D. M. and Morel, F. M. M. (2003) The bioinorganic chemistry of the ancient ocean: the co-evolution of cyanobacterial metal requirements and biogeochemical cycles at the Archean–Proterozoic boundary? *Inorg. Chim. Acta*, **356**, 308–318.

Saito, M., Moffett, J. W. and Ditullio, G. R. (2004) Cobalt and nickel in the Peru upwelling region: a major flux of labile cobalt utilized as a micronutrient. *Global Biogeochem. Cycles*, **18**, GB4030.

Saito, M. A., Rocap, G. and Moffett, J. W. (2005) Production of cobalt binding ligands in a *Synechococcus* feature at the Costa Rica upwelling dome. *Limnol. Oceanogr.*, **50**, 279–290.

Schlitzer, R. (2000) Electronic atlas of WOCE hydrographic and tracer data now available. *EOS Trans. AGU*, **81**, 45.

Selph, K. E., Landry, M. R., Taylor, A. G., Gutiérrez-Rodríguez, A., Stukel, M. R., Wokuluk, J. and Pasulka, A. L. (2016) Phytoplankton production and taxon-specific growth rates in the Costa Rica Dome. *J. Plankton Res.*, **38**, 199–215.

Sunda, W. G. and Huntsman, S. A. (1995a) Cobalt and zinc interreplacement in marine phytoplankton: biological and geochemical implications. *Limnol. Oceanogr.*, **40**, 1404–1417.

Sunda, W. G. and Huntsman, S. A. (1995b) Iron uptake and growth limitation in oceanic and coastal phytoplankton. *Mar. Chem.*, **50**, 189–206.

Vedamati, J. (2013) Comparative behavior and distribution of biologically relevant trace metals—iron, manganese, and copper in four representative oxygen deficient regimes of the world's oceans. PhD Thesis. University of Southern California.

Wang, W. X., Reinfelder, J. R., Lee, B. G. and Fisher, N. S. (1996) Assimilation and regeneration of trace elements by marine copepods. *Limnol. Oceanogr.*, **41**, 70–81.

255